

Frequency/Time-Domain Modeling of Microstrip Circuits by a Modified Spectral Domain Approach

P. Arcioni, M. Bressan, and G. Conciauro

Department of Electronics of the University of Pavia, Via Ferrata 1, I-27100 Pavia, Italy.

e-mail: arcioni@ele.unipv.it ; conciauro@ele.unipv.it

Abstract— This paper shortly describes a novel full-wave approach to the analysis of boxed planar passive MMICs. The analysis takes into account both the losses in the substrate and in the metallization. Like in the standard SDA the analysis is performed by applying the Method of the Moments in the spectral domain, but the standard algorithm is modified according to the philosophy of the Boundary-Integral Resonant-Mode-Expansion (BIRME) method. Like in frequency-time domain modeling based on Finite Difference or Finite Element methods, this modification leads to obtain the pole expansion of the admittance matrix in the *s*-plane by solving a linear matrix eigenvalue problem. With respect to finite methods the implementation of the integral approach described in this paper results in much shorter computer times and requires much smaller memory resources. One example demonstrates the advantage of the method.

I. INTRODUCTION

Many frequency- or time-domain methods are available for the full-wave analysis of passive MMICs. Using these methods a frequency- or a time-response is extrapolated from a collection of samples obtained by repeated analyses carried-out at many frequencies or times. Recently, more sophisticated methods have been proposed which lead to the simultaneous modeling in the Frequency- and Time-Domain (F/TD). In these methods a single calculation yields the mathematical model of a circuit, in the form of the pole expansion of some parameters in the *s*-domain. Any kind of frequency or time response can be deduced from this model, to any degree of resolution.

F/TD modelling is normally based on the discretization of the Maxwell equations [1] [2], which results into a state-variable formulation of the system equations. This formulation permits one to find the pole expansion of some circuit matrix by solving a linear eigenvalue problem, just as in the F/TD modelling of VLSI circuitry [3]. Some years ago, introducing a new method for the wideband modelling of 2D planar circuits [4], we presented an unusual *integral* approach which leads to a similar algorithm. Also this algorithm is based on the determination of the pole expansion by the solution of a linear eigenvalue problem; however, with respect to the aforementioned methods, it has great additional advantages in terms of computing time and memory usage.

Work partially supported by C.N.R. (MADESS II Project) under Contract no. 00.00763.PF48 and by University of Pavia, F.A.R. 2000.

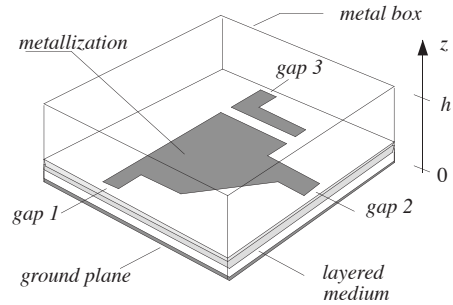


Fig. 1. A boxed microstrip circuit

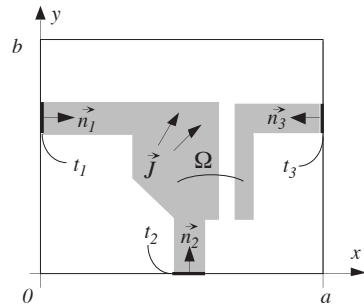


Fig. 2. Metallization and gaps

Recently, in two preliminary conference papers [5] [6], we showed that a similar philosophy can be followed for the F/TD modelling of 2.5 D multilayer microstrip circuits. In these papers we reported a simplified analysis, which assumed ideal conductors. In the present paper we outline a more refined version of the method, including the effect of conductor losses. This inclusion implies significant modifications of the theory.

II. OVERVIEW OF THE THEORY

We consider an arbitrarily shaped microstrip circuit enclosed by a conducting box (Fig. 1). The shadowed area Ω in Fig. 2 represents the metallization and includes the gaps t_1, t_2, \dots, t_K where the “gap-voltages” v_1, v_2, \dots, v_K are applied. The metallization is very thin and is embedded in a layered medium which includes some semiconducting material ($\epsilon = \epsilon_0 \epsilon_r + \sigma/j\omega$, $\mu = \mu_0$). The losses in the metalliza-

tion are taken into account by considering a sheet impedance \mathcal{Z} .

Denoting by $\vec{J} = \vec{J}(x, y)$ the current density over the metallization, the currents at the ports are given by:

$$i_k = \int_{t_k} \vec{J} \cdot \vec{n}_k dt_k \quad (k = 1, 2, \dots, K) \quad (1)$$

The tangential electric field over the region Ω satisfies:

$$\vec{E}_{\text{tang}} = - \sum_{k=1}^K v_k \delta_k(x, y) \vec{n}_k + \mathcal{Z} \vec{J}(x, y) \quad (x, y \in \Omega) \quad (2)$$

where the summation represent the field applied to the gaps (δ_k denotes a delta-function supported by t_k) and the other term is the field due to the finite conductivity of the metallization. On the other hand we can write:

$$\vec{E}_{\text{tang}} = - \sum_{n,p} Z'_{np} \tilde{J}'_{np} \vec{e}'_{np}(x, y) - \sum_{n,p} Z''_{np} \tilde{J}''_{np} \vec{e}''_{np}(x, y) \quad (3)$$

where: \vec{e}_{np} represents the (normalized) electric mode vectors of the rectangular waveguide of dimensions a, b (see Fig. 2); the prime and double prime denote quantities related to TE and TM modes, respectively; Z_{np} denotes a modal impedance of the layered waveguide, short-circuited at $z = 0$ and $z = h$, as seen from the plane of the metallization; coefficients \tilde{J}_{np} denote the spectral components of \vec{J} , with respect to mode vectors ($\tilde{J}_{np} = \int_{\Omega} \vec{J} \cdot \vec{e}_{np} dx dy$). The impedances are transcendental functions of the frequency, which can be determined either in closed form or in the form of pole expansions [7].

The spectral components of the current could be determined by the MoM solution of the equation obtained on substitution of (3) into (2). It is easily verified that, using the closed form of the impedances, this procedure is equivalent to the standard SDA.

The focal point of the modified approach described in this paper is the use of the so-called “BI-RME” representation of the field, which is obtained by introducing into (3) the pole expansion of the modal impedances. As discussed in [5] (case of two layers) and in [6] (case of many layers), we can write:

$$\begin{aligned} \vec{E}_{\text{tang}} = & - \sum_{n,p} j\omega S'_{np} \tilde{J}'_{np} \vec{e}'_{np} \\ & - \sum_{n,p} \left(R''_{np} + j\omega S''_{np} + \sum_{h=1}^H \frac{x''_{nph}}{j\omega + \xi_{nph}} \right) \tilde{J}''_{np} \vec{e}''_{np} \\ & - j\omega \sum_{n,p} \sum_C \left(a'_{npq} \sqrt{z'_{np}} + \underline{a}'_{npq} \sqrt{z'^*_{npq}} \right) \vec{e}'_{np} \\ & - j\omega \sum_{n,p} \sum_C \left(a''_{npq} \sqrt{z''_{npq}} + \underline{a}''_{npq} \sqrt{z''^*_{npq}} \right) \vec{e}''_{np} \quad (4) \end{aligned}$$

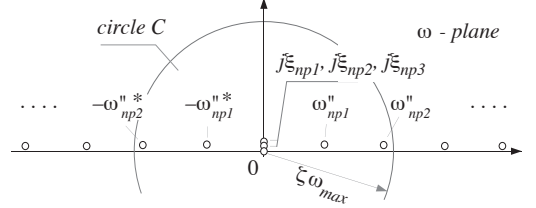


Fig. 3. Pole pattern of Z''_{np}

where:

$$\begin{aligned} a'_{npq} &= \frac{\omega \sqrt{z'_{npq}} \tilde{J}'_{np}}{\omega'_{npq} - \omega} & \underline{a}'_{npq} &= \frac{\omega \sqrt{z'^*_{npq}} \tilde{J}'_{np}}{-\omega'^*_{npq} - \omega} \\ a''_{npq} &= \frac{\omega \sqrt{z''_{npq}} \tilde{J}''_{np}}{\omega''_{npq} - \omega} & \underline{a}''_{npq} &= \frac{\omega \sqrt{z''^*_{npq}} \tilde{J}''_{np}}{-\omega''^*_{npq} - \omega} \end{aligned} \quad (5)$$

In these equations:

- the quantities (5) are the “amplitudes” of the resonant modes (TE_{npq} or TM_{npq}) of the layered box, and the pairs $(\omega_{npq}, -\omega_{npq}^*)$ are the corresponding resonating frequencies; these frequencies correspond to poles of the modal impedances and the quantities z'_{npq} and z''_{npq} are their residues; due to the losses in the medium, the poles ω_{npq} are slightly displaced upward from the real axis (Fig. 3);
- the summations denoted by Σ_C are truncated series, which take into account the only poles lying inside some circle C of radius sufficiently larger than the maximum frequency (ω_{max}) in the band of interest (Fig. 3); the accuracy of the representation (4) increases with the radius $\zeta\omega_{max}$, where ζ is an “accuracy factor” larger than 1;¹
- further poles $(j\xi_{np1}, j\xi_{np2}, \dots, j\xi_{npH})$ are placed on the imaginary axis; they belong to the modal impedances Z''_{np} and their residues are given by the real quantities x''_{np} ; their number only depends on the number of conducting layers and in all practical cases (insulating and slightly conducting layers) these poles are very close to the origin;
- $R''_{np}, S'_{np}, S''_{np}$ are real quantities, obtained by considering the first terms of the power expansion of the modal impedances around the origin [6].

The acronym “BI-RME” is used for the field representation (4), because it includes Boundary Integrals (the spectral components of \vec{J} , explicitly appearing in the first two terms) and Resonant Mode Expansions (the last two summations).

The theory of the method can be summarized as follows:
STEP 1: The current density is approximated by the formula

$$\vec{J} = \sum_{m=1}^{M'} c_m \vec{u}_m(x, y) + \sum_{m=1}^{M''} d_m \vec{w}_m(x, y) \quad (6)$$

¹It is stressed that, with increasing the order of the modes, the resonant frequencies depart from the origin and go outside of C . As a consequence, some lower-order modes only are taken into account in the summations.

where $\{\vec{u}_m\}$ and $\{\vec{w}_m\}$ are sets of suitable two-dimensional vector basis-functions defined on Ω and the weights c_m, d_m are unknown. All basis functions have zero normal component at the edges of the metallization; furthermore, functions \vec{u}_m are solenoidal ($\nabla_T \cdot \vec{u}_m = 0$), and functions $\nabla_T \cdot \vec{w}_m$ are linearly independent. We have:

$$\tilde{J}'_{np} = \sum_{m=1}^{M'} c_m \tilde{u}'_{mnp} + \sum_{m=1}^{M''} d_m \tilde{w}'_{mnp} \quad \tilde{J}''_{np} = \sum_{m=1}^{M''} d_m \tilde{w}''_{mnp}$$

where an evident symbolism is used to denote the spectral components of the basis functions with respect to TE and TM mode vectors (note that $\tilde{u}''_{mnp} = 0$).

STEP 2: Equation (4) is substituted into (2) and the resulting equation is discretized by using \vec{u}_m and \vec{w}_m as test functions (Galerkin's method). The following approximation is used:

$$\sum_{np} \sum_{h=1}^H \frac{\tilde{w}''_{\ell np} x''_{nph} \tilde{w}''_{mnp}}{j\omega + \xi_{nph}} \approx \frac{T_{\ell m}}{j\omega + \hat{\xi}_{\ell m}}$$

where:

$$T_{\ell m} = \sum_{np} \sum_{h=1}^H \tilde{w}''_{\ell np} x''_{nph} \tilde{w}''_{mnp}$$

$$\hat{\xi}_{\ell m} = \frac{1}{T_{\ell m}} \sum_{np} \sum_{h=1}^H \xi_{nph} \tilde{w}''_{\ell np} x''_{nph} \tilde{w}''_{mnp}$$

For any pair of w -functions, this approximation permits us to substitute a single pole to the cluster of poles $\{j\xi_{nph}\}$ located near the origin. The approximation is useful for reducing the order of the problem and it is very good apart from the range of very low-frequencies.

STEP 3: After introducing the auxiliary variables

$$b_\ell = \sum_{m=1}^{M''} \frac{T_{\ell m} d_m}{j\omega + \hat{\xi}_{\ell m}} \quad (7)$$

we have three sets of equations: one obtained by the Galerkin's method applied to (2), and the others obtained from (5) and (7). These equations relate the a -, b -, c - and d -variables, whose number is $N = M' + 2M'' + \text{no. of resonant frequencies included in } C$. This system can be represented by a matrix equation of the type:

$$[\mathbf{A} + \mathcal{Z}(s)\mathbf{B} - s\mathbf{C}] \mathbf{x} = \mathbf{D}\mathbf{v} \quad (s = j\omega) \quad (8)$$

where \mathbf{x} is the N -dimensional vector of the variables, and $\mathbf{A}, \mathbf{B}, \mathbf{C}, \mathbf{D}$ are matrices independent of s . $\mathbf{A}, \mathbf{B}, \mathbf{C}$ are complex symmetric matrices ($N \times N$) and \mathbf{D} is a real matrix ($N \times K$). The surface impedance is given by [8]:

$$\mathcal{Z}(s) = (s\mu_0/\sigma_m)^{1/2} \coth \left((s\mu_0\sigma_m)^{1/2} t \right) \quad (9)$$

where t and σ_m are the thickness and the conductivity of the metallization, respectively.

STEP 4: Starting from (1) and (6) we find the current vector in the form $\mathbf{i} = \mathbf{D}^T \mathbf{x}$. Then, using (8) we find the admittance matrix in the form:

$$\mathbf{Y} = \mathbf{D}^T [\mathbf{A} + \mathcal{Z}(s)\mathbf{B} - s\mathbf{C}]^{-1} \mathbf{D} \quad (10)$$

STEP 5: The inverse of the matrix is first determined by replacing the surface impedance with the low-frequency resistance $\mathcal{R} = \mathcal{Z}(0) = 1/(\sigma_m t)$. We find:

$$[\mathbf{A} + \mathcal{R}\mathbf{B} - s\mathbf{C}]^{-1} = - \sum_{n=1}^N \frac{\mathbf{x}_n^T \mathbf{x}_n}{s - \lambda_n} \quad (11)$$

where λ_n and \mathbf{x}_n are the eigenvalues and the eigenvectors obtained as solutions of the generalized linear eigenvalue equation:

$$(\mathbf{A} + \mathcal{R}\mathbf{B} - \lambda\mathbf{C}) \mathbf{x} = 0 \quad (12)$$

STEP 6: The eigenvalues laying inside the circle C (which are the most important) are corrected by a perturbation technique, to take into account the small difference between \mathcal{Z} and \mathcal{R} . The corrected eigenvalues are given by:

$$\lambda'_n = \lambda_n - [\mathcal{Z}(\lambda_n) - \mathcal{R}] \mathbf{x}_n^T \mathbf{B} \mathbf{x}_n \quad (13)$$

In conclusion we find the pole expansion of the admittance matrix:

$$\mathbf{Y} = - \sum_C \frac{\mathbf{D}^T \mathbf{x}_n^T \mathbf{x}_n \mathbf{D}}{s - \lambda'_n} - \sum_{\text{other eigenvalues}} \frac{\mathbf{D}^T \mathbf{x}_n^T \mathbf{x}_n \mathbf{D}}{s - \lambda_n} \quad (14)$$

STEP 7: Comparing (10) and (14) we obtain:

$$- \sum_{\text{other eigenvalues}} \frac{\mathbf{D}^T \mathbf{x}_n^T \mathbf{x}_n \mathbf{D}}{s - \lambda_n} \\ = \mathbf{D}^T \left([\mathbf{A} + \mathcal{Z}(s)\mathbf{B} - s\mathbf{C}]^{-1} + \sum_C \frac{\mathbf{x}_n^T \mathbf{x}_n}{s - \lambda'_n} \right) \mathbf{D}$$

Obviously, this function is analytic in C , and it can be power-expanded around the origin. If the accuracy factor is sufficiently large (e.g., $\zeta > 2.5$), the first two term of the expansion are sufficient to obtain a good approximation of the function in the frequency band of interest. We obtain:

$$\mathbf{Y} \approx - \sum_C \frac{\mathbf{D}^T \mathbf{x}_n^T \mathbf{x}_n \mathbf{D}}{s - \lambda'_n} + \mathbf{G} + s\mathbf{F} \quad (15)$$

where:

$$\mathbf{G} = \mathbf{D}^T \left[(\mathbf{A} + \mathcal{R}\mathbf{B})^{-1} - \sum_C \frac{\mathbf{x}_n^T \mathbf{x}_n}{\lambda'_n} \right] \mathbf{D}$$

$$\mathbf{F} = \mathbf{D}^T \left[(\mathbf{A} + \mathcal{R}\mathbf{B})^{-1} (\mathbf{C} - \dot{\mathcal{Z}}(0)\mathbf{B}) (\mathbf{A} + \mathcal{R}\mathbf{B})^{-1} - \sum_C \frac{\mathbf{x}_n^T \mathbf{x}_n}{\lambda_n'^2} \right] \mathbf{D}$$

($\dot{\mathcal{Z}}(0) = jt\mu_0/3$). Note that using (15) does not require the calculation of the eigensolutions of (12) outside C . The calculation of $(\mathbf{A} + \mathcal{R}\mathbf{B})^{-1}$ does not require any additional computational effort, because it is already required for the solution of (12).

III. NUMERICAL RESULTS

We used the described algorithm for the F/TD modelling of the coupled-line filter shown in Fig. 4. We considered a substrate consisting of a $100\ \mu\text{m}$ Si layer ($\epsilon_r = 11.76$, $\sigma = 1/30\ \text{S/m}$) and a $5\ \mu\text{m}$ SiO_2 layer ($\epsilon_r = 3.9$, $\sigma = 0$). The thickness of the metallization was $t = 2\ \mu\text{m}$ and its conductivity was $\sigma_m = 10^7\ \text{S/m}$. The filter was designed to feature a pass-band around 33 GHz with a 5% bandwidth. The maximum frequency of interest was 70 GHz, in order to include the first replica of the pass-band.

In the analysis we assumed an accuracy factor $\zeta = 2.5$, and we used u and w basis functions obtained as suitable combinations of rectangular rooftops [6]. We considered a total number of 241 basis functions (94 u -functions + 147 w -functions). As evidenced in Fig. 5, the results of our analysis are in very good agreement with those of a commercial solver based on a standard SDA approach (EMSSightTM, included in Microwave Office).

Our method permitted to obtain the frequency response of the filter in about 1/4 of the time required by the standard SDA, even though the numerical procedure for finding the eigenvalue was not yet optimized. Moreover, the availability of the mathematical model permitted us to plot the responses with a great detail.

In the case of a lossless metallization the BI-RME algorithm required a computer time more than one order of magnitude shorter than the time required with the standard SDA [6]. In that case some manipulations of the matrix equations permitted us to reduce substantially the order of the eigenvalue problem. We are confident that a similar procedure is possible also in the case discussed in the present paper, thus permitting us to obtain the same performance as in the lossless case.

REFERENCES

- [1] J. E. Bracken, D. K. Sun, and Z. J. Cendes, "S-domain methods for simultaneous time and frequency characterization of electromagnetic devices", *IEEE Trans on Microwave Theory Tech.*, vol. MTT 46, no. 9, Sept. 1998, pp. 1277-1290.
- [2] A. C. Cangellaris and L. Zhao, "Model order reduction techniques for electromagnetic macromodelling based on finite methods", *Int. Jour. of Numerical Modelling, Electronic Networks, Devices and Fields*, vol. 13, no. 2/3, March-June 2000, pp. 181-197.
- [3] P. Feldmann and R. W. Freund, "Efficient linear circuit analysis by Padé approximation via the Lanczos process", *IEEE Trans. Computer Aided Design*, vol. 14, May 1995, pp. 639-649.
- [4] P. Arcioni, M. Bressan, and G. Conciauro, "A new algorithm for the wideband analysis of arbitrarily shaped planar circuits", *IEEE Trans on Microwave Theory Tech.*, vol. MTT-36, n. 10, Oct. 1988, pp. 1426-1437.
- [5] P. Arcioni, M. Bressan, G. Conciauro, and A. R. Olea Garcia, "BI-RME Modeling of Passive Structures for Silicon MMICs: Feasibility and Results", II Topical Meeting on Silicon Monolithic Integrated Circuits in RF Systems, April 26-28, 2000 Garmisch, Germany.
- [6] P. Arcioni, M. Bressan, G. Conciauro, and A. R. Olea Garcia, "New Ideas for Frequency/Time Domain Modeling of Passive Structures for MMICs", Europ. Congr. on Computational Methods in Applied Sciences and Eng., *ECCOMAS 2000*, Barcelona, Sept. 11-14, 2000.
- [7] G. Conciauro and M. Bressan, "Singularity Expansion of Mode Voltages and Currents in a Layered, Anisotropic, Dispersive Medium Included between Two Ground Planes", *IEEE Trans. on Microwave Theory Tech.*, vol. MTT-47, no. 9, Sept. 1999, pp. 1617-1626.
- [8] E. Palenczy, D. Kinowski, J. F. Legier, P. Pribetich and P. Kennis, "Comparison of Full Wave Approaches for Determination of Microstrip Conductor Losses for MMIC Applications" *Electronic Letters*, Vol. 26, No. 25, Dec. 6, 1990, pp. 2076-2077.

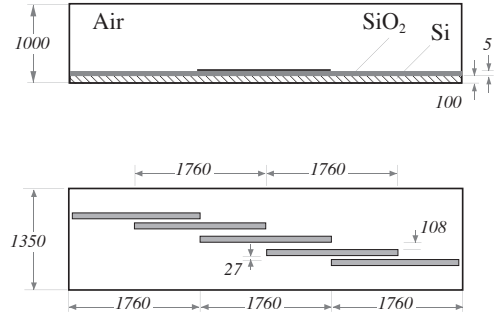


Fig. 4. A microstrip coupled-line filter (dimensions in μm)

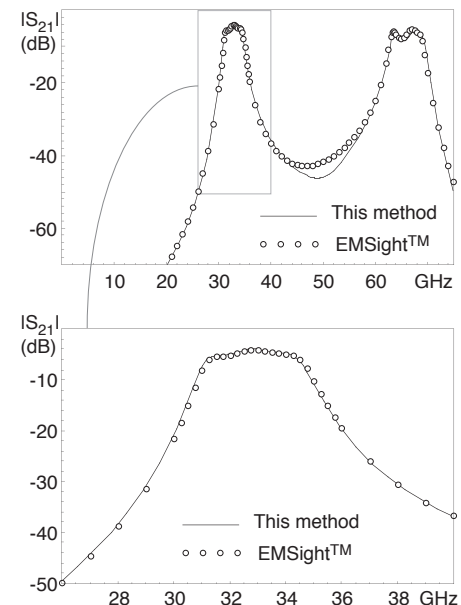


Fig. 5. Frequency response of the filter of Fig. 4.